

How to simulate global cosmic strings with large string tension

Vincent B. Klaer, Guy D. Moore

*Institut für Kernphysik, Technische Universität Darmstadt
Schlossgartenstraße 2, D-64289 Darmstadt, Germany*

E-mail:

vklaer@theorie.iikp.physik.tu-darmstadt.de, guy.moore@physik.tu-darmstadt.de

ABSTRACT: Global string networks may be relevant in axion production in the early Universe, as well as other cosmological scenarios. Such networks contain a large hierarchy of scales between the string core scale and the Hubble scale, $\ln(f_a/H) \sim 70$, which influences the network dynamics by giving the strings large tensions $T \simeq \pi f_a^2 \ln(f_a/H)$. We present a new numerical approach to simulate such global string networks, capturing the tension without an exponentially large lattice.

KEYWORDS: axions, dark matter, cosmic strings, global strings

Contents

1	Introduction	1
2	How to get large string tensions in a global model	4
3	Numerical implementation and results	10
3.1	Numerical implementation	10
3.2	Results	13
4	Discussion and conclusions	17

1 Introduction

Cosmic strings are extended solitonic objects which arise in field theories when a symmetry G is broken, $G \rightarrow H$, and the quotient space G/H has nontrivial π_1 homotopy [1–3]. The simplest example is when a complex scalar field $\varphi = \frac{\varphi_r + i\varphi_i}{\sqrt{2}}$ possesses a U(1) symmetry, $\varphi \rightarrow e^{i\theta_A}\varphi$, but the potential leads to spontaneous symmetry breaking,¹

$$-\mathcal{L} = \partial_\mu\varphi^*\partial^\mu\varphi + \frac{m^2}{8v^2}\left(2\varphi^*\varphi - f_a^2\right)^2. \quad (1.1)$$

Here m is the mass of the radial (Higgs) excitation and f_a is the vacuum value of the scalar field. Under this Lagrangian, the vacuum state is of form $\varphi = \sqrt{2}f_a e^{i\theta_A}$, and the arbitrary angle θ_A breaks the U(1) symmetry completely. If the field initially makes this choice of symmetry breaking direction randomly and independently at widely separated points in space, then the initial conditions generically contain string type defects (the Kibble mechanism [1]). Qualitatively, the same lessons are true if φ is charged under a U(1) gauge symmetry. We will refer to the case with gauge symmetry as a theory of local or abelian strings, and the theory where the U(1) symmetry is a global symmetry as a theory of global or scalar-only strings.

If a network of such defects exists in the Universe, it could influence the development of cosmic structure [4–6]. A more physically interesting scenario, in light of strong limits on the role of strings in cosmic structure [7–10], is the possibility that the QCD axion [11, 12] makes up the Dark Matter of the Universe [13–15]. The QCD axion’s Lagrangian is the same as Eq. (1.1), with the addition of a small temperature-dependent explicit symmetry breaking term $\chi(T)(\cos[\text{Arg}\varphi] - 1)$, which becomes important around the QCD scale. If the axion field starts out with randomly different values for the symmetry-breaking angle θ_A at different space points, which is plausible and maybe even likely [16], then there would be an initial network of (axionic) global cosmic strings. This network is destroyed around

¹We use natural units and $[-+++]$ metric signature.

the QCD scale when the potential's tilt becomes important, but it could play a dominant role in establishing the density of axions produced [17].

If we could understand the efficiency of axion production in the early Universe, then assuming the axion makes up the dark matter, we could predict the axion mass [16]. The problem is that we don't understand the string network evolution well enough. There is no consensus in the literature for the efficiency of axion production [18–35]. Recent large-scale numerical simulations [35, 36] have not resolved this problem, because no simulation to date can correctly treat the tension of a global string. As we will now explain, numerical simulations of global string networks typically study networks where the strings have a tension $\mathcal{O}(10)$ times smaller than the physically relevant value. This may be dramatically misrepresenting the density, longevity, and role of the strings in these simulations, and therefore the amount of axions produced [36].

To understand the problem, consider the field solution for a string under the Lagrangian of Eq. (1.1). Choosing the string to lie along the z axis in polar coordinates (z, r, ϕ) , the string solution is

$$\varphi(z, r, \phi) = e^{i\phi} f(mr) f_a \sqrt{2}, \quad (1.2)$$

$$f''(x) = -\frac{x f'(x) + f(x)}{x^2} - \frac{f(x)(1 - f(x)^2)}{2}, \quad (1.3)$$

$$f(0) = 0, \quad \lim_{x \rightarrow \infty} f(x) = 1.$$

Here we have shown the differential equation and boundary values which the radial function $f(mr)$ should obey. This solution should be valid out to a value of r of order the distance to the next string, which is parametrically $Hr \sim 1$ (with H the Hubble parameter). In terms of the parameter $x = mr$, this is a value of $x \sim m/H \gg 1$. For instance, for an axion near the QCD scale, $H \sim T^2/m_{\text{pl}} \sim 10^{-19}$ GeV while $m \sim f_a \sim 10^{11}$ GeV (for a typical estimate of f_a [37]). To see why this is a problem for simulations, we estimate the energy per length, or tension T , stored in the string:

$$T = \int_0^{2\pi} d\phi \int_0^{\sim H^{-1}} r dr \left[\frac{1}{2} |\partial_r \varphi|^2 + \frac{1}{2r^2} |\partial_\phi \varphi|^2 \right] \quad (1.4)$$

$$\simeq 2\pi \int_{\sim m^{-1}}^{\sim H^{-1}} r dr \frac{1}{2r^2} f_a^2 \simeq \pi f_a^2 \ln \frac{m}{H} \equiv \pi f_a^2 \kappa.$$

The string tension is logarithmically small- r divergent, because the derivative in the ϕ direction is proportional to $1/r$. Therefore the tension contains a logarithmically large factor $\ln(m/H)$, which for the values quoted above is $\ln(10^{30}) \simeq 70$. If the goal is to study global strings playing a role in structure formation in the modern Universe, and they arise from a GUT or other high-scale theory, then the logarithm may be more like $\ln(10^{15} \text{ GeV} \times 10^{10} \text{ year}) \sim 113$. We have named the magnitude of this logarithm κ .

On the other hand, existing numerical simulations of global string networks rely on modifying Eq. (1.1) to incorporate Hubble expansion, in comoving coordinates and conformal time, and solving it numerically as a function of (conformal) time on a spatial lattice. To properly treat the string defects, it is necessary that the lattice resolves the string cores,

that is, the lattice spacing a must satisfy $ma \lesssim 1$. At the same time, the lattice box-size must be larger than the typical inter-string spacing, and is typically larger by a factor of at least a few. Therefore, in the numerical simulation, the ratio of string separation-to-core is constrained to be at most a few hundred, and the logarithm of interest is at most 5 or 6. In other words, in existing simulations [33, 36], the global strings have a string tension at least an order of magnitude too small.

Does this matter? Probably it does. Global string networks differ from the much better-studied local string networks [19, 38–42] in two important ways:

1. There is a massless field coupled to the string, namely the Goldstone boson mode θ_A (the phase of φ). The strings can radiate away their energy to this field. The strength of the interaction is governed by f_a^2 . Radiation should make it easier for strings to lose energy, leading to a less-dense network of smoother strings.
2. The massless field also communicates inter-string forces. These could help the strings to find each other and annihilate, again leading to a smaller string density. The strength of the interactions is again governed by f_a^2 .

These effects compete against string-tension effects which scale as $T = \pi\kappa f_a^2$. Therefore the global-string effects are suppressed by a factor of $1/\kappa$, and are ~ 10 times *less* important in true string network evolutions than in those which we can simulate.

We know that these effects play a major role in string network evolution, because the density of the string network in global string simulations is about a factor of 4–8 smaller than in local string network simulations [25, 39–43]. Therefore, the correct inclusion of the high tension of string cores may lead to a substantial change in the string network dynamics and the network density. Indeed, in the *limit* $\kappa \gg 1$, we expect the global string networks to become indistinguishable from local strings. Probably $\kappa = 70$ is not enough to achieve this limit, but it should certainly give different string dynamics than $\kappa = 5$. In the context of axion production, the denser network with a larger string tension means there is more energy available for the production of axions. But the large tension makes the strings more robust to external forces, so the network should be more persistent once the potential tilts, and will take longer to annihilate away.

It is difficult to extrapolate the consequences of the high string tension on axion production [35]. Therefore, a method to simulate global string networks with $\kappa \sim 70$ is clearly well motivated. One of us recently presented such a method and implemented it in 2 space dimensions [44]. The results indicated that the produced axion density rises rather modestly with string tension. However, 2 dimensions may show quite different physics than 3, and we have not (yet) been able to extend the method proposed in [44] to 3 space dimensions. Instead, in this paper we will propose another approach to simulate a global string network with enhanced string core tension. Essentially, we will present a model in which each global string has an abelian-Higgs string bound onto its core. The abelian Higgs string provides most of the string tension, and the long-range interactions are controlled by the global Goldstone fields. The ratio of tensions is tunable and can be chosen to make $\kappa \sim 70$ without much difficulty. The next section, Section 2, explains the model which

does this and justifies that the relevant infrared physics should be correct. We study the resulting string networks numerically in Section 3, and present a discussion and conclusions in Section 4. Very briefly, we find that as κ is increased, the resulting string network grows denser and its properties (velocity, cusps) change from those of a global network towards those of an abelian-Higgs network. Applications to axion production are postponed to a follow-up paper.

2 How to get large string tensions in a global model

We are interested in the large-scale structure of string networks and the infrared behavior of any (pseudo)Goldstone modes they radiate. For these purposes it is not necessary to keep track of all physics down to the scale of the string core. Rather, it is sufficient to describe the desired IR behavior with an *effective theory* of the strings and the Goldstone modes around them. This consists of removing the physics very close to the string core with an equivalent set of physics. It has long been known how to do this [19]. The string cores are described by the Nambu-Goto action [45–47], which describes the physics generated by the string tension arising close to the string core. The physics of the Goldstone mode is described by a Lagrangian containing the scalar field’s phase. And they are coupled by the Kalb-Ramond action [48, 49]:

$$\mathcal{L} = \mathcal{L}_{\text{NG}} + \mathcal{L}_{\text{GS}} + \mathcal{L}_{\text{KR}}, \quad (2.1)$$

$$\mathcal{L}_{\text{NG}} = \kappa\pi f_a^2 \int d\sigma \sqrt{y'^2(\sigma)(1 - \dot{y}^2(\sigma))}, \quad (2.2)$$

$$\mathcal{L}_{\text{GS}} = f_a^2 \int d^3x \partial_\mu \theta_A \partial^\mu \theta_A, \quad (2.3)$$

$$\mathcal{L}_{\text{KR}} = \int d^3x A_{\mu\nu} j^{\mu\nu}, \quad (2.4)$$

$$H_{\mu\nu\alpha} = f_a \epsilon_{\mu\nu\alpha\beta} \partial^\beta \theta_A = \partial_\mu A_{\nu\alpha} + \text{cyclic}, \quad (2.5)$$

$$j^{\mu\nu} = -2\pi f_a \int d\sigma (v^\mu y'^\nu - v^\nu y'^\mu) \delta^3(x - y(\sigma)). \quad (2.6)$$

Here σ is an affine parameter describing the string’s location $y^\mu(\sigma, t)$, $v^\mu = (1, \dot{y}) = dy^\mu/dt$ is the string velocity, and $H_{\mu\nu\alpha}$ and $A_{\mu\nu}$ are the Kalb-Ramond field strength and tensor potential, which are a dual representation of θ_A . Effectively \mathcal{L}_{NG} tracks the effects of the string tension, which we name $\kappa\pi f_a^2$, stored locally along its length. Next, \mathcal{L}_{GS} says that the axion angle propagates under a free wave equation, as expected for a Goldstone boson, and its decay constant is f_a . And \mathcal{L}_{KR} incorporates the interaction between strings and axions, also controlled by f_a . The interaction can be summarized by saying that the string forces θ_A to wind by 2π in going around the string (in the same sense that the $eJ_\mu A^\mu$ interaction in electrodynamics can be summarized by saying that it enforces that the electric flux emerging from a charge is e).

It should be emphasized that in writing these equations, we are implicitly assuming a separation scale r_{min} ; at larger distances from a string $r > r_{\text{min}}$ we consider $\nabla\varphi$ energy to

be associated with θ_A ; for $r < r_{\min}$ the gradient energy is considered as part of the string tension [19].

Any other set of UV physics which reduces to the effective description of Eq. (2.1) would present an equally valid way to study this string network. Our plan is to find a model without a large scale hierarchy, such that the IR behavior is also described by Eq. (2.1) with a large value for the string tension. Optimally, we want a model which is easy to simulate on the lattice with a spacing not much smaller than r_{\min} . Reading Eq. (2.2) through Eq. (2.6) in order, the model must have Goldstone bosons with a decay constant f_a and strings with a large and tunable tension $T = \kappa \pi f_a^2$, with $\kappa \gg 1$. There can be other degrees of freedom, but only if they are very heavy (with mass $m \sim r_{\min}^{-1}$), and we will be interested in the limit that their mass goes to infinity. Finally, the string must have the correct Kalb-Ramond charge. Provided everything is derived from an action, this will be true if the Goldstone boson mode always winds by 2π around a loop which circles a string.

We do this by writing down a model of two scalar fields φ_1, φ_2 , each with a U(1) phase symmetry. A linear combination of the phases is gauged; specifically, the fields are given electrical charges $q_1 \in \mathcal{Z}$ and $q_2 = q_1 - 1$ under a single U(1) gauge field. The orthogonal phase combination represents a global U(1) symmetry which will give rise to our Goldstone bosons. The role of the gauge symmetry will be to attach an abelian-Higgs string onto every global string, which will enhance the string tension. The added degrees of freedom are all massive off the string, achieving our intended effective description.

Specifically, the Lagrangian is

$$\begin{aligned}
-\mathcal{L}(\varphi_1, \varphi_2, A_\mu) &= \frac{1}{4e^2} F_{\mu\nu} F^{\mu\nu} + \left| (\partial_\mu - iq_1 A_\mu) \varphi_1 \right|^2 + \left| (\partial_\mu - iq_2 A_\mu) \varphi_2 \right|^2 \\
&+ \frac{m_1^2}{8v_1^2} \left(2\varphi_1^* \varphi_1 - v_1^2 \right)^2 + \frac{m_2^2}{8v_2^2} \left(2\varphi_2^* \varphi_2 - v_2^2 \right)^2 \\
&+ \frac{\lambda_{12}}{2} \left(2\varphi_1^* \varphi_1 - v_1^2 \right) \left(2\varphi_2^* \varphi_2 - v_2^2 \right). \tag{2.7}
\end{aligned}$$

For simplicity we will specialize to the case

$$\lambda_{12} = 0, \quad m_1 = m_2 = \sqrt{e^2(q_1^2 v_1^2 + q_2^2 v_2^2)} \equiv m_e. \tag{2.8}$$

The model has 6 degrees of freedom; two from each scalar and two from the gauge boson. Symmetry breaking, $\varphi_1 = e^{i\theta_1} v_1 \sqrt{2}$ and $\varphi_2 = e^{i\theta_2} v_2 \sqrt{2}$, spontaneously breaks both U(1) symmetries and leaves five massive and one massless degrees of freedom. Specifically, expanding about a vacuum configuration, the fluctuations and their masses are

$$v_1 \rightarrow v_1 + h_1, \quad m = m_1 \tag{2.9}$$

$$v_2 \rightarrow v_2 + h_2, \quad m = m_2 \tag{2.10}$$

$$A_i \neq 0, \quad m = \sqrt{e^2(q_1^2 v_1^2 + q_2^2 v_2^2)} \equiv m_e \tag{2.11}$$

$$(\theta_1, \theta_2) \rightarrow (\theta_1, \theta_2) + \omega(q_1, q_2), \quad \text{eaten by } A \tag{2.12}$$

$$(\theta_1, \theta_2) \rightarrow (\theta_1, \theta_2) + \theta_A \left(\frac{q_2}{q_1^2 + q_2^2}, \frac{-q_1}{q_1^2 + q_2^2} \right) \quad m = 0. \tag{2.13}$$

We see that the choices in Eq. (2.8) have made all heavy masses equal.² To clarify, note that a gauge transformation $A_\mu \rightarrow A_\mu + \partial_\mu \omega$ changes $\theta_1 \rightarrow \theta_1 + q_1 \omega$ and $\theta_2 \rightarrow \theta_2 + q_2 \omega$. Therefore the linear combination of θ_1, θ_2 fluctuations with $\delta\theta_1 \propto q_1$ and $\delta\theta_2 \propto q_2$ is precisely the combination which can be shifted into A^μ by a gauge change, and is therefore the combination which is “eaten” by the A -field to become the third massive degree of freedom. The remaining phase difference $q_2\theta_1 - q_1\theta_2$ is gauge invariant,

$$q_2\theta_1 - q_1\theta_2 \rightarrow_\omega q_2(\theta_1 + q_1\omega) - q_1(\theta_2 + q_2\omega) = q_2\theta_1 - q_1\theta_2 + 0\omega \quad (2.14)$$

and represents a global, Goldstone-boson mode.

The model breaks two U(1) symmetries, so we must describe strings in terms of a double (m, n) representing the winding number of each scalar field around the string. In the absence of gauge interactions (for $e \rightarrow 0$) the φ_1, φ_2 fields would not interact and the tension of the $(1, 1)$ string would be the sum of the tensions of a $(1, 0)$ and a $(0, 1)$ string. Therefore the $(1, 1)$ string would be neutrally stable to splitting into $(1, 0)$ and $(0, 1)$ strings. Gauge interactions strongly change this, such that $(1, 0)$ and $(0, 1)$ strings strongly attract and $(1, 1)$ strings are stable. To show this we analyze the form of a (j, k) string. For the *Ansatz*

$$\begin{aligned} \sqrt{2}\varphi_1(r, \phi) &= e^{ij\varphi} f_1(r)v_1, \\ \sqrt{2}\varphi_2(r, \phi) &= e^{ik\varphi} f_2(r)v_2, \\ A_\phi(r) &= \frac{g(r)}{r}, \end{aligned} \quad (2.15)$$

we find the equations of motion from Eq. (2.7) are

$$g'' - \frac{g'}{r} = e^2 v_1^2 f_1^2 q_1 (q_1 g - j) + e^2 v_2^2 f_2^2 q_2 (q_2 g - k), \quad (2.16)$$

$$f_1'' + \frac{f_1'}{r} = \frac{f_1}{r^2} (j - q_1 g)^2 + \frac{m^2}{2} f_1 (f_1^2 - 1), \quad (2.17)$$

$$f_2'' + \frac{f_2'}{r} = \frac{f_2}{r^2} (k - q_2 g)^2 + \frac{m^2}{2} f_2 (f_2^2 - 1). \quad (2.18)$$

Here f_1, f_2 represent the progress of the two scalar fields towards their large-radius asymptotic vacuum values, while $2\pi g(r)$ is the magnetic flux enclosed by a loop at radius r , which trends at large r towards the total enclosed magnetic flux. The large- r behavior is well behaved only if $f_1 \rightarrow 1, f_2 \rightarrow 1$, and

$$\lim_{r \rightarrow \infty} g(r) = \frac{j q_1 v_1^2 + k q_2 v_2^2}{q_1^2 v_1^2 + q_2^2 v_2^2} = \frac{1}{2\pi} (\text{enclosed magnetic flux}). \quad (2.19)$$

²We set $\lambda_{12} = 0$ so that the fluctuations in $|\varphi_1|$ and $|\varphi_2|$ are unmixed; our other choices ensure that all heavy fields have the same mass. We could consider other cases but we see no advantage in doing so if the goal is to implement the model on the lattice. The lattice spacing is limited by the inverse of the heaviest particle mass, while the size of the string core and the mass of extra degrees of freedom off the string will be set by the inverse of the lightest particle mass. So we get a good continuum limit with the thinnest strings, and therefore the best resolution of the network, by having all heavy masses equal.

The magnetic flux is therefore a compromise between the value j/q_1 , which cancels large-distance gradient energies for the first field, and k/q_2 , which cancels large-distance gradient energies for the second field. Unless $q_2j - q_1k = 0$, the gradient energies are not canceled at long distance. Indeed, we can understand the difference $(q_2j - q_1k)$ as the global (axionic) charge of the string. The gradient energy at large distance is given by

$$\begin{aligned} T &\simeq 2\pi \int r dr (|D_\phi \varphi_1|^2 + |D_\phi \varphi_2|^2) \\ &\simeq \pi \int r dr \left(\frac{v_1^2}{r^2} (j - q_1 g)^2 + \frac{v_2^2}{r^2} (k - q_2 g)^2 \right) \\ &\simeq \pi \int \frac{dr}{r} \frac{v_1^2 v_2^2 (jq_2 - kq_1)^2}{q_1^2 v_1^2 + q_2^2 v_2^2}, \end{aligned} \quad (2.20)$$

which is proportional to the squared global charge of the string. Naming $q_{\text{global}} = jq_2 - kq_1$, comparing Eq. (1.4) with Eq. (2.20), we identify the Goldstone-mode decay constant as

$$f_a^2 = \frac{v_1^2 v_2^2}{q_1^2 v_1^2 + q_2^2 v_2^2}. \quad (2.21)$$

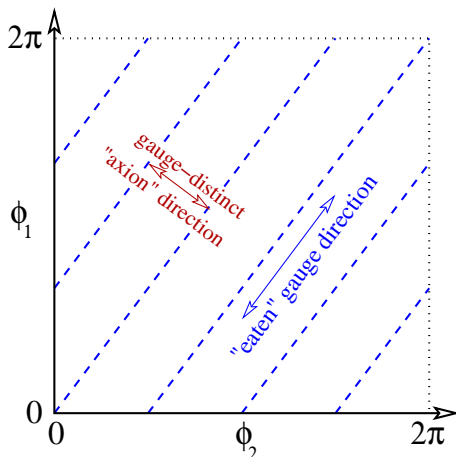


Figure 1. Space of φ_1, φ_2 phases (θ_1, θ_2) for the case $(q_1, q_2) = (4, 3)$. The dashed (blue) line indicates phase pairs which are equivalent under gauge transformations. An appropriate vector potential can cancel any gradient energy in the direction of the dashed lines.

Because q_1 and q_2 are of the same sign, the resulting large-distance energy is smaller for the $(1, 1)$ string than for the sum of the $(1, 0)$ and $(0, 1)$ strings, and therefore there is an attractive interaction between $(1, 0)$ and $(0, 1)$ strings, which like to bind into a $(1, 1)$ string. Alternatively we could say that the global charge of the $(1, 0)$ string is q_2 and the $(0, 1)$ string is $-q_1$, so they are strongly attracted by the Goldstone-mediated interaction and bind into a $(1, 1)$ string.

For a more intuitive explanation, consider Figure 1. It shows the set of possible phases (θ_1, θ_2) for the two scalar fields, in the case $(q_1, q_2) = (4, 3)$. The figure includes a dotted line to indicate which phase choices are gauge-equivalent. Moving along the dotted

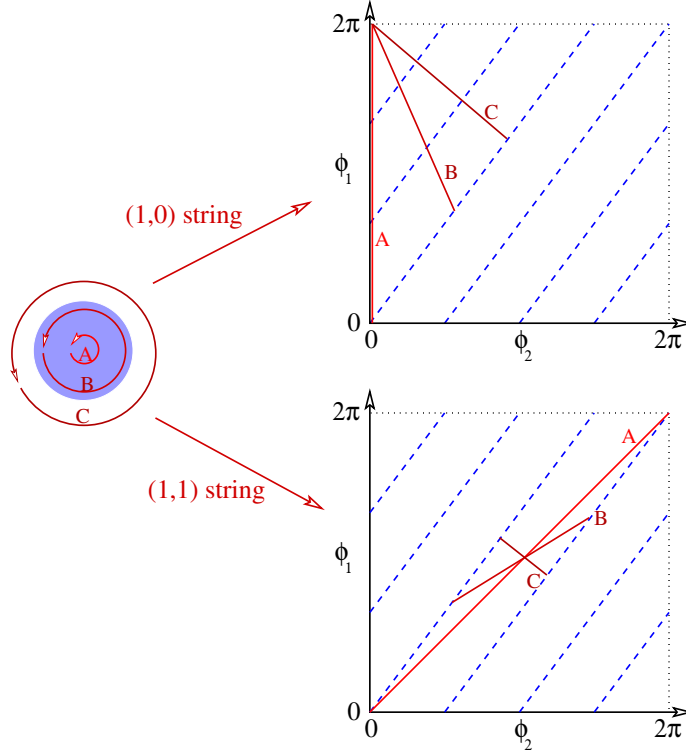


Figure 2. Left: cross-section of a string, showing the magnetic field strength “bundle” and three possible loops one can take around the center of the string. Right: path through (ϕ_1, ϕ_2) space taken along each loop, for a $(1,0)$ string (top) and a $(1,1)$ string (bottom). As more magnetic flux is enclosed, the component of $(\Delta\theta_1, \Delta\theta_2)$ along the gauge-direction is canceled, but the component in the “global” direction is not. This component is small for the $(1,1)$ string.

line corresponds to changing the gauge, or moving through space along a gauge field; a vector potential of the right size can cancel a gradient energy along this field direction. The orthogonal direction, which is unaffected by a gauge field, is the global (axion) field direction. A change in this direction from one blue dotted line to the next represents a full 2π rotation in the (axial) Goldstone direction, which explains the value of f_a found in Eq. (2.21). Figure 2 then shows how gradient energies behave in a $(1,0)$ or $(1,1)$ string. As the scalar field value varies around a loop, the gradient energy in the dotted-blue direction is partly canceled by A_ϕ gauge field. The extent of cancellation depends on the enclosed flux. As one goes from a small loop within the string core to a large loop outside the core, more and more of the scalar gradient along the dotted-line direction is canceled by the enclosed flux. For the innermost loop there is no enclosed flux, and the gradient energy is given by the distance between the point $(\theta_1, \theta_2) = (0,0)$ to the point $(2\pi, 0)$ or $(2\pi, 2\pi)$ for the $(1,0)$ or the $(1,1)$ string respectively. For a loop enclosing the entire flux, all gradient energy arising from the gauge-direction is canceled. This nearly completely removes the gradient energy for the $(1,1)$ string, but the reduction is modest for the $(1,0)$ string. Therefore the $(1,1)$ string has a small gradient energy outside the core, representing a small residual coupling to the (axion) Goldstone field, but the $(1,0)$ string has a large gradient energy

and a large coupling.

For our simulation to correspond with the global string model, it should have Goldstone modes between a network of strings with charge-1 under the Goldstone fields. That is, we want a network of (1, 1) strings only, with no other string types. Because the (1, 1) string is stable, achieving this is simply a matter of choosing the right initial conditions. We choose θ_1 randomly and independently at each point, $A_\mu = 0 = E_i = \dot{\varphi}_1 = \dot{\varphi}_2$ initially, and $\theta_2 = \theta_1$. In this case only (1, 1) strings are present initially, and the network never develops any other sort of string or structure. Since $q_2\theta_1 - q_1\theta_2$ is initially random, there are no long-range correlations in the Goldstone field and the Kibble mechanism ensures a network of (1, 1) strings, whose evolution should approach the scaling behavior of a network with a tension set by the (1, 1) string tension and the Goldstone mode interaction strength found above. Our initial conditions also obey Gauss' Law, which is then preserved by the evolution.

Now let us estimate the effective value of κ , the ratio of the string tension to the string interaction via Goldstone modes, for such a (1, 1) string. The energy of the string's core is the energy of an abelian Higgs string with $m_h = m_e$ and with $f^2 = v_1^2 + v_2^2$, which is

$$T_{\text{abelian}} \simeq \pi(v_1^2 + v_2^2). \quad (2.22)$$

The value of κ is therefore

$$\kappa = \frac{T}{\pi f_a^2} \simeq \frac{v_1^2 + v_2^2}{\frac{v_1^2 v_2^2}{q_1^2 v_1^2 + q_2^2 v_2^2}} = \frac{(v_1^2 + v_2^2)(q_1^2 v_1^2 + q_2^2 v_2^2)}{v_1^2 v_2^2} \xrightarrow{v_1=v_2} 2(q_1^2 + q_2^2). \quad (2.23)$$

This is not quite correct; the solution only coincides with the abelian-Higgs solution for large $q_1 \gg 1$. For finite q_1 we must compute the true solution, and account for the $1/r^2$ tail of energy arising from the long-distance Goldstone-mode content of the string. Therefore we solve Eq. (2.16), Eq. (2.17), Eq. (2.18) numerically by multiparameter shooting to establish the string solution and its energy. Artificially separating the short and long distance energy contributions by choosing $r_{\min} = \pi/m$ and writing the energy-per-length stored in fields out to radius R as

$$T_R = \int_0^R \frac{dT}{dr} dr \equiv (\bar{\kappa} + \ln(mR/\pi)) \pi f_a^2, \quad (2.24)$$

(or equivalently, $\bar{\kappa} = \lim_{R \rightarrow \infty} T_R/\pi f_a^2 - \ln mR/\pi$), we find the values of κ shown in Table 1. The table shows that Eq. (2.23) is quite accurate, for our choice of r_{\min} . For future use, the table also records the small-distance behavior of f_1 , f_2 , and g , defined as

$$\begin{aligned} f_1(r) &= c_1 m r + \mathcal{O}(r^3), \\ f_2(r) &= c_2 m r + \mathcal{O}(r^3), \\ g(r) &= d(mr)^2 + \mathcal{O}(r^4). \end{aligned} \quad (2.25)$$

Note that all results in the table are for the case of equal masses and equal vacuum values; we could achieve $\bar{\kappa}$ values intermediate between those shown by considering asymmetric vacuum values $v_1 > v_2$.

q_1	q_2	$\bar{\kappa}$	c_1	c_2	d
5	4	82.290	0.618084	0.582967	0.0547499
4	3	50.288	0.621225	0.576319	0.0697357
3	2	26.283	0.625697	0.563648	0.0954803
2	1	10.267	0.630809	0.532107	0.1476050

Table 1. Numerical value of extra string tension $\bar{\kappa}$, and small-distance behaviors of radial functions, for several charge combinations.

To summarize, the model of Eq. (2.7) has an infrared description consisting of one Goldstone mode and strings. The strings have a tension $\kappa\pi f_a^2$ with tunable κ given by Eq. (2.23). The Goldstone phase winds by 2π in circling the string, so the Kalb-Ramond charge of the string is correct. This description breaks down at a scale $m_1 = m_2$, which is both the scale setting the thickness of the string and the scale of massive excitations off the strings. The model can be implemented numerically with only a little more work than the abelian-Higgs model.

3 Numerical implementation and results

3.1 Numerical implementation

For an FRW spacetime in comoving coordinates and conformal time, the action is

$$S = \int_0^1 dt \int d^3x t^k \mathcal{L}[\text{Eq. (2.7)}] \quad (3.1)$$

where k is determined by the expansion rate; $k = 2$ for radiation (which we will study), $k = 4$ for matter, *etc.*³ Our approach is to write a spacetime-lattice discretization of the action and to determine the update rule by extremization of this action. This leads automatically to a leapfrog update rule. We use noncompact formulation of U(1), recording gauge fields $A_i(x)$ (which “live” on links) directly and computing link variables

$$U_i(x) = P \exp \int_x^{x+a\hat{i}} -iA_i dl = e^{-iaA_i(x)} \quad (3.2)$$

when needed. We use an a^2 improved action, both for the scalar fields and the gauge fields. To our knowledge this has not been done correctly before in simulating abelian Higgs fields for cosmic string networks. Our implementation is almost the same as a previous attempt to a^2 -improve the abelian Higgs mechanism [50], except that we correctly modify the electric field part, see below. The improved scalar field “hopping” term is (4/3) times a

³For an FRW universe with equation of state $P = w\varepsilon$, $k = 4/(1 + 3w)$.

nearest-neighbor term minus (1/12) a next-nearest neighbor term,

$$S_{\nabla\varphi} = \sum_{t=\delta n_t a} \sum_{x=a\vec{n}_x} \left[\sum_{i=1,2,3} t^k \left(\frac{4|U_i^q(x,t)\varphi(x+a\hat{i},t) - \varphi(x,t)|^2}{3} - \frac{|U_i^q(x,t)U_i^q(x+a\hat{i},t)\varphi(x+2a\hat{i},t) - \varphi(x,t)|^2}{12} \right) - (t + \delta a/2)^k \frac{|U_0^q(x,t)\varphi(x,t + \delta a) - \varphi(x,t)|^2}{\delta^2} \right], \quad (3.3)$$

with q the charge for the specific field considered, and δ the ratio of temporal to spatial discretization; we typically use $\delta = 1/6$ which is adequate [36]. In practice we fix to temporal gauge, $U_0 = 1$, which is numerically convenient but not very relevant as long as we ask only gauge invariant questions.

The noncompact magnetic field action is (5/3) a square plaquette term minus (1/12) a sum on rectangular plaquettes (the abelian version of the tree-level a^2 improved or Symanzik action [51, 52]),

$$S_B = \sum_{t,x,i>j} \frac{5t^k}{6e^2} \left(A_i(x) + A_j(x+a\hat{i}) - A_i(x+a\hat{j}) - A_j(x) \right)^2 - \sum_{t,x,i\neq j} \frac{t^k}{24e^2} \left(A_i(x) + A_i(x+a\hat{i}) + A_j(x+2a\hat{i}) - A_i(x+a[\hat{i}+\hat{j}]) - A_i(x+a\hat{j}) - A_j(x) \right)^2 \quad (3.4)$$

while the electric field action is

$$S_E = - \sum_{t,x,i} (t+a\delta/2)^k \left[\frac{2}{3} \frac{(A_i(x,t+\delta a) - A_i(x,t))^2}{\delta^2} - \frac{1}{24} \frac{(A_i(x,t+a\delta) + A_i(x+a\hat{i},t+a\delta) - A_i(x,t) - A_i(x+a\hat{i},t))^2}{\delta^2} \right]. \quad (3.5)$$

This last modification, explained in detail in [53], is necessary to make the evolution truly improved – for instance, without it the gauge boson dispersion relation has a^2 corrections. Unfortunately it causes the A -field update to be implicit. To see this, first define $E_i(x,t) = A_i(x,t+a\delta) - A_i(x,t)$. Then S_E can be written as $\sum_{x,i} (7/12)E_i^2(x) - (1/12)E_i(x)E_i(x+a\hat{i})$. Because the Lagrangian is not simply diagonal in the $E \sim \dot{A}$, there is a difference between the time derivative of A and the canonical momentum of A . It is convenient to define the quantity $P_i(x) = -(1/12)E_i(x-a\hat{i}) + (7/6)E_i(x) - (1/12)E_i(x+a\hat{i})$, which in the continuous-time limit is the canonical momentum of the A field. Its time-update is simple, but the relation between P and E must be inverted to update the A field. Because the relation is nearly diagonal, this inversion can be done perturbatively and proves not to be a large

numerical overhead.⁴ (In Ref. [53] this was the dominant cost, because the reference works with SU(2) where E is a gauge non-singlet and parallel transportation is involved in inverting the E - P relation.)

Improvement increases the operation count by roughly a factor of 2.5, and most of the update effort is spent on the scalar field update. We have implemented the resulting equations of motion in c using MPI and AVX2, obtaining 2×10^7 site updates per second on an i5core duo (two physical cores), and with MPI and AVX512, obtaining 5×10^8 site updates per second on a compute node with 2 64-core KNL Xeon Phi processors communicating through Infiniband. A 2048^3 lattice fits in approximately 512G of memory. Relative to the simple complex-scalar model of Eq. (1.1), the memory demand is $3.5\times$ as large and the compute time is $6\times$ larger on the Xeon Phi and $16\times$ larger on the i5core.

We identify the plaquettes pierced by a string using the gauge-invariant definition of Kajantie *et al* [54], applied to one of the fields (we use φ_1). We measure string velocity by a slight generalization of the method of Ref. [36]; we use the small- r expansion of $f_1(r)$:

$$f_1(r) = c_1 mr + e_1 (mr)^3 + \dots \quad e_1 = -\frac{c_1(1 + 4q_1 d)}{16}, \quad (3.6)$$

and we use the string velocity estimate that near the center of a string core, [36]

$$\gamma^2 v^2 = \frac{|\partial_t \phi|^2}{2m^2 c_1^2 v^2} \left(1 - \frac{4e_1 \phi^* \phi}{c_1^2 v^2} \right) - \frac{4e_1 (\varphi^* \partial_t \varphi + \varphi \partial_t \varphi^*)^2}{m^2 c_1^4 v^4} + \mathcal{O} \left(\frac{\varphi^4 (\partial_t \varphi)^2}{m^2 v^6} \right), \quad (3.7)$$

which should converge to the correct velocity in the small- a limit as $(ma)^4$.⁵ The values of c_1 and d are in Table 1. For each plaquette pierced by a string, we average $\gamma^2 v^2$ over the plaquette's four corners, and use this average to determine v, γ . Finally, we interpolate the position within a plaquette where the string pierces it, by fixing to the gauge where each link is $\pm 1/4$ the value of the magnetic flux through the plaquette, and interpolating the φ_1 field to find its zero [55]. We construct strings as the series of straight segments connecting these interpolating points [55]. The overhead to identify and record strings is a small fraction of the numerical effort. We have compared the results using the other field φ_2 for string identification, and consistently find string length and mean velocity to agree within 1%. We also check the average distance between a point on the φ_2 string network and the nearest point on the φ_1 string network: for $q_1 = 4$ and $mt = 512$ we find an average distance of $0.065/m$. Therefore each scalar describes essentially the same string network; in particular our procedure for getting only (1, 1) type strings is successful.

⁴This procedure can be thought of as putting a tridiagonal matrix M , with diagonal elements $[-1/12, 7/6, -1/12]$, in the Hamiltonian for a column of E -fields in one direction, $H(E) = \sum_i EME/2$. An alternative with a simpler update would be to define N a tridiagonal matrix with diagonal elements $[+1/12, 5/6, +1/12]$ and to use $H(E) = EN^{-1}E/2$. These are equivalent at order a^2 . In the latter case we would have $P = N^{-1}E$ or $E = NP$. One then stores and updates P , and easily generates $E = NP$ when needed to perform the A -field update. No matrix inversions are required. In each case the energy in electric fields is determined from $\sum_x E_i P_i/2$. We did not implement this procedure, but we would use it if we were writing the code from new.

⁵There are other estimators, such as that used in Ref. [43], which may be less spacing-sensitive at the spacing we consider. It would be interesting to compare them systematically. One virtue of our choice is that $v < 1$ is manifest, since one computes $\gamma^2 v^2$ rather than v directly.

3.2 Results

We will present some very preliminary results obtained on $2048 \times 2016 \times 2000$ lattices with relatively coarse spacing $ma = 1$. We compare the 2-scalar model at a few values of q_1 with the abelian-Higgs model on the one hand, and a scalar-only global model on the other. In each case we take $ma = 1.0$, except for the scalar-only model, which has thicker strings relative to the mass (c_1 of Eq. (2.25) is $c_1 = 0.412$) and which is therefore less sensitive to the mass value. Therefore for the scalar-only case we used $ma = 1.5$. We have not extrapolated to finer lattice spacing, which will in particular lead to a larger mean string velocity than what we report below. Our main goals are to show that the numerics are relatively straightforward to conduct, and that many properties of the string networks evolve smoothly from their behavior in the global theory with low tension towards the behavior observed in local (abelian-Higgs) networks as the string tension is increased. But not all at the same rate; the string velocity shifts rather quickly, while the network density takes a much larger tension to become more abelian-Higgs-like. We intend to make a more comprehensive study in the future.

We will focus on the density of the string network, the mean string velocity, and how “cuspy” the strings are. The general expectation is that the network should evolve towards a scaling solution, where the density of strings and other string properties scale with the system age (see for instance [56, 57]). We introduce the scaled network density ξ and mean inter-string distance L_{sep} , defined as

$$L_{\text{sep}}^{-2} \equiv V^{-1} \int_{\text{all string}} \gamma dl, \quad \xi \equiv \frac{t^2}{(1 + k/2)^2 L^2}. \quad (3.8)$$

Here $\int \gamma dl$ is the invariant string length, V is the space volume and t the time, all in co-moving conformal coordinates. The factor $(1 + k/2)^{-2}$ converts from conformal-time based to physical-time based normalization, which is common usage in some of the literature. Note that different authors define the string density in different ways, often with the same symbol. For instance, a recent study of abelian-Higgs networks⁶ [43, 58] uses the symbol ξ to represent the quantity we call L_{sep} .

We will also consider the orientation autocorrelator of the string; defining \vec{s} as the unit tangent vector of the string, this is defined as⁷

$$D(\Delta l) = \frac{\int_{\text{all string}} \vec{s}(l) \cdot \vec{s}(l + \Delta l) dl}{\int_{\text{all string}} dl}; \quad (3.9)$$

more details will be given in a future publication [55].

Our goal is to understand the scaling behavior of string networks, and how it depends on κ . In practice we will never precisely observe scaling, and in some cases we may be quite far away. Three effects can cause scaling violations at a finite time t ;

⁶Our abelian-Higgs simulations are generally in good agreement with this reference, but the reference is much more systematic, and achieves higher statistics and better extrapolation towards the continuum.

⁷Note that we have used rest-frame string lengths without γ factors in this definition. This can be improved but we have not yet done so.

1. Scaling occurs when the string core has negligible size compared to the inter-string spacing. Therefore it is difficult for the network to show good scaling at early times, before $mt \gg 1$.
2. The string tension does have a residual contribution from the Goldstone field, which increases as the string separation increases with time. Since the mean inter-string spacing is expected to grow linearly with time, we expect $\kappa(t) \simeq \kappa(t_0) + \ln(t/t_0)$.
3. Initial conditions may start the network out as denser or thinner than the scaling form, and it takes time for the network to adjust.

The severity of the first problem should scale as $(mt)^{-1}$ and therefore becomes less severe as we achieve larger lattices which can be run to later times⁸ (and if we can use coarser grids, $ma \sim 1$, which is why we use an improved action). But the severity of this problem also depends on how *cuspy* the strings are – how much fine structure there is along a string. After all, such cusps can occur on much smaller scales than the inter-string spacing, and we expect that any cusp structure on scales smaller than roughly the string thickness will be lost to heavy-mode radiation, which is unphysical from the viewpoint of the thin-string limit. Cusps should tend to dissipate through Goldstone mode radiation. Parametrically, because radiation involves πf_a^2 while the energy available is set by the tension $\pi \kappa f_a^2$, string features with length scale l should dissipate in time $t \sim l\kappa$. Therefore smaller- κ strings should lose their short-scale structure, and the necessary separation-to-core hierarchy should scale roughly linearly with κ . So larger- κ networks should demand larger lattices and later times before correct scaling sets in.

The second problem is most severe when the κ contribution from our abelian degrees of freedom is small; for larger q -values the Abelian contribution overwhelms any small scale-dependence in the Goldstone contribution. Therefore this problem is mostly an issue for purely global simulations, and perhaps for $(q_1, q_2) = (2, 1)$.

The issue of initial conditions requires that, if we want to say with any confidence that we are close to scaling, we need to see a variety of network initial conditions, with different initial string densities, converge to a common string density. As stated above, we take as initial conditions that $A_i = 0$ and $\varphi_1 = v_1 e^{i\theta_1(x)}$, $\varphi_2 = v_2 e^{i\theta_1(x)}$ (same phase as φ_1) at time $t = 0$ – actually at time $t = a$ with a the lattice spacing. This choice leads however to a string network which starts out quite dilute compared to the scaling solution. Therefore we modify the evolution by setting $k = k_{\text{start}}$ until some time t_{start} . A large value of k_{start} represents strongly overdamped evolution, leading to slow string motion and a much denser starting network, without excessive fluctuations. By varying k_{start} and t_{start} , we can vary the early-time density of the string network.

Figure 3 shows how the network density varies with the string tension. For each type of network, we have run two groups of simulations, one which starts with a somewhat underdense network ($k_{\text{start}} = 20$ and $t_{\text{start}} = 40$) and one which starts with a somewhat overdense network ($k_{\text{start}} = 50$ and $t_{\text{start}} = 80$ except for the abelian-Higgs case, where we

⁸We stop the evolution at $t = L/2$, L the box length, to ensure that the lattice’s periodicity is invisible under causal dynamics.

used $k_{\text{start}} = 80$ and $t_{\text{start}} = 100$). In every case the different densities converge towards each other with time. While many authors consider only the length of “long” strings, neglecting short loops, our results are based on summing over all string lengths. However, in all of our simulations, small loops make up a relatively small fraction of the total string length; for each simulation type, we find that loops satisfying $\int \gamma dl < 2\pi L_{\text{sep}}$ make up less than 10% of the total string length. This might seem surprising for the abelian Higgs case if one compares against expectations from Nambu-Goto simulations [39, 40] but it is consistent with recent lattice field-theory findings [43, 58]. This difference, along with the factor-2 difference in density of long strings between Nambu-Goto simulations and lattice field-theory simulations, probably arises because the Nambu-Goto simulations are sensitive to very short-scale phenomena which cannot be resolved even with the largest field theoretical simulations to date [59].

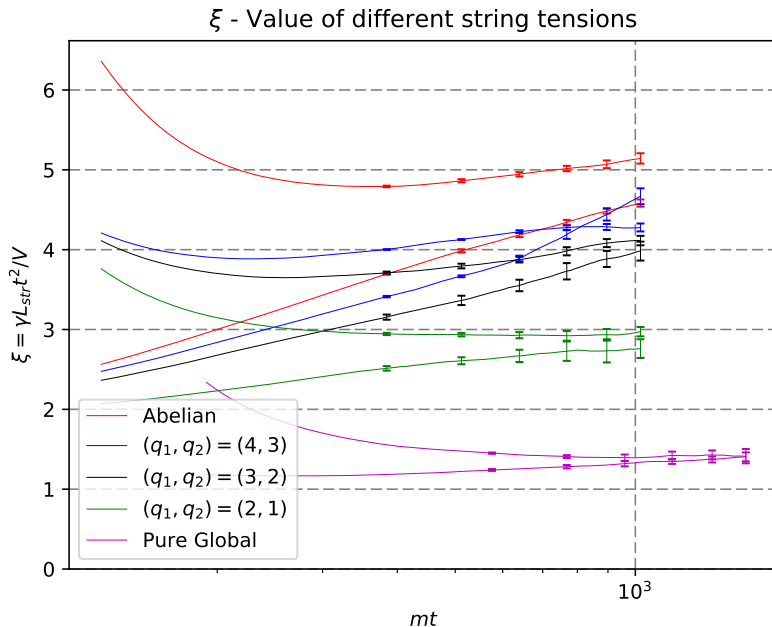


Figure 3. Network density for different string tensions. The falling curves represent the overdense networks, while the rising curves represent the underdense networks.

The lowest density network is for pure scalar-field simulations. The densest network is for abelian-Higgs networks. Increased-tension networks fall in between, with the network density increasing as one increases the string tension. The figure indicates that the string density increases more slowly than linearly with κ . For the lower-tension networks it appears that ξ converges to a good late-time value. However for the highest-tension networks and the abelian Higgs case, it appears that ξ continues to grow at the largest available times; indeed, when the network is initialized as overdense, ξ first falls, but then bottoms out and rises, which clearly indicates that the dynamics are not free of finite $1/(mt)$ corrections – that is, we are not in the large-time limit for these networks. This fits with

our expectations that, the larger the value of κ , the larger the mt value must be before small-scale structure is well resolved in the simulation.

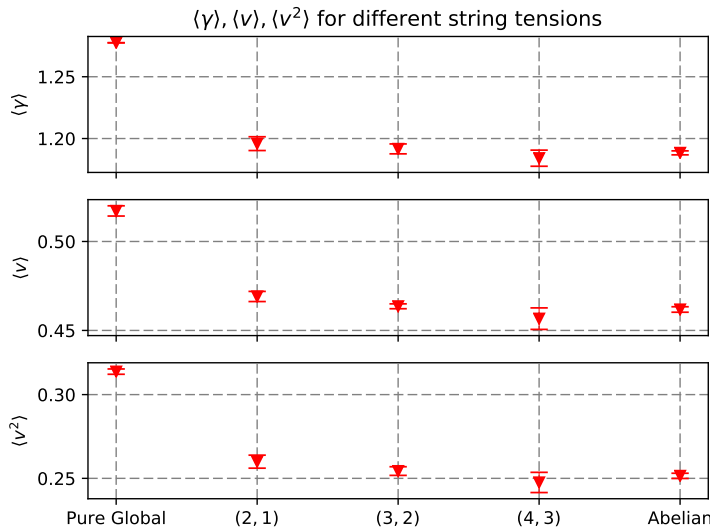


Figure 4. Mean gamma factor $\langle \gamma \rangle$, velocity $\langle v \rangle$ and squared velocity $\langle v^2 \rangle$. The upper and lower bar indicates the mean values for the overdense network (upper) and for the underdense network (lower).

Figure 4 shows the mean string velocity, squared velocity, and gamma factor, each defined as

$$\left. \begin{array}{l} \langle v \rangle \\ \langle v^2 \rangle \\ \langle \gamma \rangle \end{array} \right\} \equiv \frac{\int \gamma dl \times \begin{cases} v \\ v^2 \\ \gamma \end{cases}}{\int \gamma dl}. \quad (3.10)$$

For the overdense network the mean values are always slightly higher than for the underdense network; the difference exceeds the statistical error in either measurement. Therefore, rather than statistical error bars, we have plotted the mean values of the overdense and underdense network for the latest time we achieved, $mt = 1024$. We stress that the velocity measurements are not extrapolated to the continuum (in the sense of small ma); preliminary indications are that all values will rise when we do so. However the qualitative feature, that the scalar-only theory has a higher velocity and that it then comes down rather quickly towards the abelian-Higgs value as the string tension is increased, appears to be robust.

Figure 5 shows the string-direction autocorrelator for each string type. The x -axis is a separation distance along a string, normalized by the system age. That is, an x -axis value of $\ell/t = 0.2$ means that we consider all pairs of points (x, y) separated along a string by $\int_x^y dl = 0.2t$. The y -axis is the dot product of their unit tangent vectors. We see that the strings with a larger coupling to Goldstone modes are systematically straighter (larger correlator) than the strings with smaller or no Goldstone coupling. The effect is

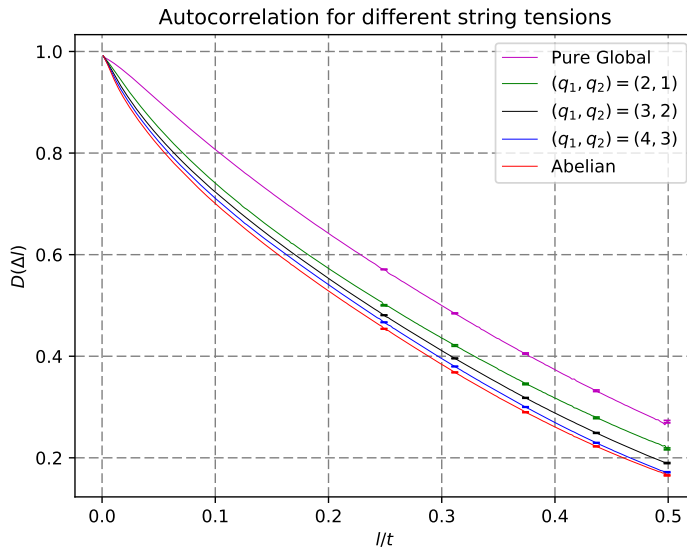


Figure 5. Autocorrelation of the string-direction for different string tensions.

especially clear at very small separation. A string consisting only of smooth curves would have vanishing slope at $\ell/t = 0$, while a string with perfectly sharp cusps would have a nonzero slope at $\ell/t = 0$ set by the density and angle of the cusps. This cuspy behavior is consistent with the abelian-Higgs curve, but not with the scalar-only curve. Enhanced-tension strings lie in between, though closer to the abelian-Higgs case. We expect that the abelian-Higgs string and the highest-tension 2-field strings are not yet displaying their large- mt asymptotic behavior.

4 Discussion and conclusions

We have presented a new algorithm for simulating global string networks, which makes it possible to consider networks with a large value of κ , the ratio of the string tension to the coupling to Goldstone modes. This makes it possible to simulate global string networks with a very large hierarchy between the Hubble scale and the microscopic string core scale, without actually resolving the hierarchy numerically. Preliminary numerical studies find that high-tension global strings behave similarly to abelian Higgs networks, for the lattice sizes we have achieved. In particular we very clearly see that the density of string networks smoothly increases from the value observed in scalar-only simulations towards the value observed in abelian Higgs simulations, as the string tension is increased. Physically, we expect that the needed lattice resolution to properly capture small scale string structure should grow linearly with κ , meaning that large lattices are needed. But with our approach, the lattice size need only grow as the *logarithm* of f_a/H , not with f_a/H itself.

Our approach has clear applications to the physics of axion production in the early Universe. We have shown that existing simulations must underestimate the network density, because they fail to capture the larger string tension. Roughly, existing axion simulations

are comparable to the scalars-only curve in Figure 3, while the physical tension is somewhat above the $(4, 3)$ line in the figure – which itself is probably not yet scaling, but should display a still higher network density. Therefore the string density in simulations of axion production is underestimated by at least a factor of 3. This could certainly be important in establishing axion production. The large difference in string tension could also be important. Therefore one should revisit the question of axion production from axionic string network breakup, using our approach. We intend to do so in the near future. It might also be interesting to revisit the study of the possible role of global cosmic strings in cosmology.

Acknowledgments

We thank the Technische Universität Darmstadt and its Institut für Kernphysik, where this work was conducted. We thank Kari Rummukainen and David Weir for fruitful and interesting conversations, as well as conversations with Neil Turok, a very long time ago. We especially thank Mark Hindmarsh; conversations with Mark inspired this method, although we doubt he realizes it.

References

- [1] T. W. B. Kibble. Topology of Cosmic Domains and Strings. *J. Phys.*, A9:1387–1398, 1976.
- [2] Alexander Vilenkin. Cosmic Strings and Domain Walls. *Phys. Rept.*, 121:263–315, 1985.
- [3] G. W. Gibbons, S. W. Hawking, and T. Vachaspati, editors. *The Formation and evolution of cosmic strings. Proceedings, Workshop, Cambridge, UK, July 3-7, 1989*, 1990.
- [4] Ya. B. Zeldovich. Cosmological fluctuations produced near a singularity. *Mon. Not. Roy. Astron. Soc.*, 192:663–667, 1980.
- [5] A. Vilenkin. Cosmological Density Fluctuations Produced by Vacuum Strings. *Phys. Rev. Lett.*, 46:1169–1172, 1981. [Erratum: *Phys. Rev. Lett.*46,1496(1981)].
- [6] T. W. B. Kibble. Some Implications of a Cosmological Phase Transition. *Phys. Rept.*, 67:183, 1980.
- [7] P. A. R. Ade et al. Planck 2013 results. XXV. Searches for cosmic strings and other topological defects. *Astron. Astrophys.*, 571:A25, 2014.
- [8] Jon Urrestilla, Neil Bevis, Mark Hindmarsh, and Martin Kunz. Cosmic string parameter constraints and model analysis using small scale Cosmic Microwave Background data. *JCAP*, 1112:021, 2011.
- [9] Joanes Lizarraga, Jon Urrestilla, David Daverio, Mark Hindmarsh, Martin Kunz, and Andrew R. Liddle. Constraining topological defects with temperature and polarization anisotropies. *Phys. Rev.*, D90(10):103504, 2014.
- [10] Andrei Lazanu, E. P. S. Shellard, and Martin Landriau. CMB power spectrum of Nambu-Goto cosmic strings. *Phys. Rev.*, D91(8):083519, 2015.
- [11] Steven Weinberg. A New Light Boson? *Phys.Rev.Lett.*, 40:223–226, 1978.
- [12] Frank Wilczek. Problem of Strong p and t Invariance in the Presence of Instantons. *Phys.Rev.Lett.*, 40:279–282, 1978.

- [13] John Preskill, Mark B. Wise, and Frank Wilczek. Cosmology of the Invisible Axion. *Phys. Lett.*, B120:127–132, 1983.
- [14] L. F. Abbott and P. Sikivie. A Cosmological Bound on the Invisible Axion. *Phys. Lett.*, B120:133–136, 1983.
- [15] Michael Dine and Willy Fischler. The Not So Harmless Axion. *Phys. Lett.*, B120:137–141, 1983.
- [16] L. Visinelli and P. Gondolo. Axion cold dark matter in view of BICEP2 results. *Phys. Rev. Lett.*, 113:011802, 2014.
- [17] Richard Lynn Davis. Cosmic Axions from Cosmic Strings. *Phys. Lett.*, B180:225, 1986.
- [18] R. L. Davis and E. P. S. Shellard. Do Axions Need Inflation? *Nucl. Phys.*, B324:167, 1989.
- [19] Atish Dabholkar and Jean M. Quashnock. Pinning Down the Axion. *Nucl. Phys.*, B333:815, 1990.
- [20] C. Hagmann and P. Sikivie. Computer simulations of the motion and decay of global strings. *Nucl. Phys.*, B363:247–280, 1991.
- [21] R. A. Battye and E. P. S. Shellard. Global string radiation. *Nucl. Phys.*, B423:260–304, 1994.
- [22] R. A. Battye and E. P. S. Shellard. Radiative back reaction on global strings. *Phys. Rev.*, D53:1811–1826, 1996.
- [23] Sanghyeon Chang, C. Hagmann, and P. Sikivie. Studies of the motion and decay of axion walls bounded by strings. *Phys. Rev.*, D59:023505, 1999.
- [24] Masahide Yamaguchi, Jun’ichi Yokoyama, and M. Kawasaki. Numerical analysis of formation and evolution of global strings in $(2+1)$ -dimensions. *Prog. Theor. Phys.*, 100:535–545, 1998.
- [25] Masahide Yamaguchi, M. Kawasaki, and Jun’ichi Yokoyama. Evolution of axionic strings and spectrum of axions radiated from them. *Phys. Rev. Lett.*, 82:4578–4581, 1999.
- [26] Masahide Yamaguchi. Scaling property of the global string in the radiation dominated universe. *Phys. Rev.*, D60:103511, 1999.
- [27] Masahide Yamaguchi, Jun’ichi Yokoyama, and M. Kawasaki. Evolution of a global string network in a matter dominated universe. *Phys. Rev.*, D61:061301, 2000.
- [28] C. Hagmann, Sanghyeon Chang, and P. Sikivie. Axion radiation from strings. *Phys. Rev.*, D63:125018, 2001.
- [29] C. J. A. P. Martins, J. N. Moore, and E. P. S. Shellard. A Unified model for vortex string network evolution. *Phys. Rev. Lett.*, 92:251601, 2004.
- [30] Olivier Wantz and E.P.S. Shellard. Axion Cosmology Revisited. *Phys.Rev.*, D82:123508, 2010.
- [31] Takashi Hiramatsu, Masahiro Kawasaki, and Ken’ichi Saikawa. Evolution of String-Wall Networks and Axionic Domain Wall Problem. *JCAP*, 1108:030, 2011.
- [32] Takashi Hiramatsu, Masahiro Kawasaki, Toyokazu Sekiguchi, Masahide Yamaguchi, and Jun’ichi Yokoyama. Improved estimation of radiated axions from cosmological axionic strings. *Phys.Rev.*, D83:123531, 2011.
- [33] Takashi Hiramatsu, Masahiro Kawasaki, Ken’ichi Saikawa, and Toyokazu Sekiguchi. Production of dark matter axions from collapse of string-wall systems. *Phys.Rev.*, D85:105020, 2012.

- [34] Takashi Hiramatsu, Masahiro Kawasaki, Ken'ichi Saikawa, and Toyokazu Sekiguchi. Axion cosmology with long-lived domain walls. *JCAP*, 1301:001, 2013.
- [35] Masahiro Kawasaki, Ken'ichi Saikawa, and Toyokazu Sekiguchi. Axion dark matter from topological defects. *Phys.Rev.*, D91(6):065014, 2015.
- [36] Leesa Fleury and Guy D. Moore. Axion dark matter: strings and their cores. *Journal of Cosmology and Astroparticle Physics*, 2016(01):004, 2016.
- [37] Giovanni Grilli di Cortona, Edward Hardy, Javier Pardo Vega, and Giovanni Villadoro. The QCD axion, precisely. *JHEP*, 01:034, 2016.
- [38] Andreas Albrecht and Neil Turok. Evolution of Cosmic String Networks. *Phys. Rev.*, D40:973–1001, 1989.
- [39] David P. Bennett and Francois R. Bouchet. High resolution simulations of cosmic string evolution. *Phys. Rev.*, D41:2408, 1990.
- [40] Bruce Allen and E. P. S. Shellard. Cosmic string evolution: a numerical simulation. *Phys. Rev. Lett.*, 64:119–122, 1990.
- [41] Vitaly Vanchurin, Ken Olum, and Alexander Vilenkin. Cosmic string scaling in flat space. *Phys. Rev.*, D72:063514, 2005.
- [42] Ken D. Olum and Vitaly Vanchurin. Cosmic string loops in the expanding Universe. *Phys. Rev.*, D75:063521, 2007.
- [43] Mark Hindmarsh, Joanes Lizarraga, Jon Urrestilla, David Daverio, and Martin Kunz. Scaling from gauge and scalar radiation in Abelian Higgs string networks. 2017.
- [44] Leesa M. Fleury and Guy D. Moore. Axion String Dynamics I: 2+1D. *JCAP*, 1605(05):005, 2016.
- [45] Tetsuo Goto. Relativistic quantum mechanics of one-dimensional mechanical continuum and subsidiary condition of dual resonance model. *Prog. Theor. Phys.*, 46:1560–1569, 1971.
- [46] P. Goddard, J. Goldstone, C. Rebbi, and Charles B. Thorn. Quantum dynamics of a massless relativistic string. *Nucl. Phys.*, B56:109–135, 1973.
- [47] Yoichiro Nambu. Strings, Monopoles and Gauge Fields. *Phys. Rev.*, D10:4262, 1974.
- [48] Michael Kalb and Pierre Ramond. Classical direct interstring action. *Phys. Rev.*, D9:2273–2284, 1974.
- [49] Alexander Vilenkin and Tanmay Vachaspati. Radiation of Goldstone Bosons From Cosmic Strings. *Phys. Rev.*, D35:1138, 1987.
- [50] Mark Hindmarsh, Kari Rummukainen, Tuomas V. I. Tenkanen, and David J. Weir. Improving cosmic string network simulations. *Phys. Rev.*, D90(4):043539, 2014. [Erratum: *Phys. Rev.* D94, no. 8, 089902(2016)].
- [51] P. Weisz. Continuum Limit Improved Lattice Action for Pure Yang-Mills Theory. 1. *Nucl. Phys.*, B212:1–17, 1983.
- [52] G. Curci, P. Menotti, and G. Paffuti. Symanzik's Improved Lagrangian for Lattice Gauge Theory. *Phys. Lett.*, 130B:205, 1983. [Erratum: *Phys. Lett.* 135B, 516(1984)].
- [53] Guy D. Moore. Improved Hamiltonian for Minkowski Yang-Mills theory. *Nucl. Phys.*, B480:689–728, 1996.

- [54] K. Kajantie, M. Karjalainen, M. Laine, J. Peisa, and A. Rajantie. Thermodynamics of gauge invariant U(1) vortices from lattice Monte Carlo simulations. *Phys. Lett.*, B428:334–341, 1998.
- [55] Vincent B. Klaer and Guy D. Moore. Global string networks and the one-scale model (in preparation).
- [56] C. J. A. P. Martins and E. P. S. Shellard. Quantitative string evolution. *Phys. Rev.*, D54:2535–2556, 1996.
- [57] C. J. A. P. Martins and E. P. S. Shellard. Extending the velocity dependent one scale string evolution model. *Phys. Rev.*, D65:043514, 2002.
- [58] David Daverio, Mark Hindmarsh, Martin Kunz, Joanes Lizarraga, and Jon Urrestilla. Energy-momentum correlations for Abelian Higgs cosmic strings. *Phys. Rev.*, D93(8):085014, 2016. [Erratum: *Phys. Rev.* D95,no.4,049903(2017)].
- [59] J. N. Moore, E. P. S. Shellard, and C. J. A. P. Martins. On the evolution of Abelian-Higgs string networks. *Phys. Rev.*, D65:023503, 2002.